Progressive Integrality Outer–Inner Approximation for AC Unit Commitment with Conic Formulation

Yongzheng Dai

ISyE, Georgia Institute of Technology, Atlanta, GA, USA

Abstract

The alternating-current unit commitment (AC-UC) problem provides a realistic representation of power system operations, which is a nonconvex mixed-integer nonlinear programming problem and hence is computationally intractable. A common relaxation to the AC-UC is based on the second-order cone (SOC), which results in a mixed-integer second-order cone program and remains computationally challenging. In this paper, we propose an outer-inner approximation framework that alternatively solves a mixed-integer linear programming (MILP) as an outer approximation and a convex second-order cone programming as an inner approximation to find a (near-)optimal solution to the SOC-based AC-UC. To improve computational efficiency, we introduce a progressive integrality strategy that gradually enforces integrality, reducing the reliance on expensive MILP solutions in early iterations. In addition, time-block Benders cuts are incorporated to strengthen the outer approximation and accelerate convergence. Computational experiments on large-scale test systems, including 200-bus and 500-bus networks, demonstrate that the proposed framework significantly improves both efficiency and robustness compared to state-of-the-art commercial solvers. The results show faster convergence, higher-quality solutions, and improved scalability under different formulations and perturbed load scenarios.

Nomenclature

(1) Sets and Indexes:	
$\mathcal{T}$	Time periods, $\mathcal{T} := \{1, ..., T\}$.
$\mathcal{G}$	Generating units, $\mathcal{G} := \mathcal{G}^{\mathrm{T}} \cup \mathcal{G}^{\mathrm{R}}$.
$\mathcal{G}^{\mathrm{T}}$	Thermal generating units.
$\mathcal{G}^{\mathrm{R}}$	Weather-dependent renewable generating units.

$\mathcal{N}$	Nodes in the electric network.
$\mathcal{R}$	Reliability Areas.
Ω_r	Generating units in the reliability area r.
$\mathcal{E}$	Transmission lines.
Λ_n	Adjacent nodes to node n.
Λ_n^{G}	Generating units at node n.
(2) Constants:	
C_g^{F}	Fixed cost of unit g.
$C_g^{\mathrm{SU}}/C_g^{\mathrm{SD}}$	Startup/shutdown cost of unit g.
C_g^{V}	Variable cost of unit g.
C^{P}	Penalty cost for unserved or over-produced power.
L_g/F_g	Initial up/down time of thermal generating unit g.
$T_g^{\mathrm{U}}/T_g^{\mathrm{D}}$	Minimum up/down time of thermal generating unit g.
$p_g^{\min}/p_g^{\max}$	Minimum/maximum active power output from unit g.
$q_g^{\min}/q_g^{\max}$	Minimum/maximum reactive power output from unit g.
$u_{g,0}, y_{g,0}, z_{g,0}$	Status at the beginning of the scheduling of unit g.
$p_{g,0}$	Initial active power output of unit g.
$R_g^{\mathrm{U}}/R_g^{\mathrm{SD}}$	Up/startup ramping limit of unit g.
$R_g^{\mathrm{D}}/R_g^{\mathrm{SD}}$	Down/shutdown ramping limit of unit g.
$R_{r,t}^{\mathrm{D}}$	Reserve required in reliability area r in period t.
$S_{n,m}$	Capacity of line (m,n).
$G_{n,m}/B_{n,m}$	Conductance/susceptance of line (m,n).
$b_{n,m}^{\mathrm{shunt}}$	Half of the shunt susceptance of line (m,n).
$V_n^{\max}/V_n^{\min}$	Maximum/minimum voltage level for node n.
$p_{n,t}^{\mathrm{D}}/q_{n,t}^{\mathrm{D}}$	Active/reactive power demand in period t and node n.
T	Number of stages.
(3) Variables:	
$u_{g,t}$	On/off status in period t of unit g.
$y_{g,t}$	Startup indicator in period t of unit g.
$z_{g,t}$	Shutdown indicator in period t of unit g.
$p_{g,t}/q_{g,t}$	Active/reactive power produced by unit g in period t.
$\bar{p}_{g,t}$	Maximum available active power output in period t from unit g.
$p_{n,m,t}/q_{n,m,t}$	Active/reactive power flow of line (n,m) in period t.
$p_{n,t}^{\mathrm{U}}/q_{n,t}^{\mathrm{U}}$	Unserved active/reactive load in period t and node n.
$p_{n,t}^{\mathrm{O}}/q_{n,t}^{\mathrm{O}}$	Over-produced active/reactive load in period t and node n.
$c_{n,m,t}, s_{n,m,t}$	Auxiliary variables for the second-order-conic formulation.

1 Introduction

The unit commitment problem is a central task in the short-term power system planning, determining the on/off status and generation levels of power units over a planning horizon. Traditionally, the unit commitment problems are solved using direct-current (DC) approximations of power flow, which can be formulated as a mixed-integer linear programming (MILP) [Carrión and Arroyo, 2006, Conejo and Baringo, 2018]. However, DC-based unit commitment relies on linearized DC power flow, ignoring reactive power, voltage magnitudes, and losses [Wood et al., 2013], and may therefore yield commitment schedules that are infeasible or require significant corrective actions when evaluated under full alternating-current (AC) laws [Bai et al., 2015, Molzahn et al., 2019]. As modern power systems become increasingly stressed and incorporate more renewable generation, accurately modeling AC network constraints has become essential.

Incorporating AC power flow equations into UC leads to the alternating-current unit commitment (AC-UC) problem, which is a highly nonconvex mixed-integer nonlinear programming (MINLP) problem [Frangioni et al., 2008]. To address this issue, convex relaxation techniques for AC power flow, including semidefinite programming (SDP) [Lavaei and Low, 2011] and second-order cone (SOC) relaxations [Jabr, 2006], have been applied to UC, leading to MISOCP formulations of AC-UC. These methods provide tighter relaxations and stronger optimality guarantees. However, solving large-scale MISDPs or MISOCPs remains computationally challenging, as they involve both nonlinear network constraints and discrete commitment decisions [Bonami et al., 2011, Gally et al., 2018].

An abundance of techniques have been studied to solve unit commitment, which can be categorized into several classes. The first class is the decomposition methods, including Lagrangian relaxation (LR) methods [Muckstadt and Koenig, 1977, Zhuang and Galiana, 2002], Benders decomposition, and other related decompositions [Nasri et al., 2015, Constante-Flores and Conejo, 2024]. The LR method decomposes the MISOCP into smaller subproblems and has been widely studied for large-scale AC-UC. However, LR approaches often produce infeasible solutions for the original problem and require additional heuristics for feasibility recovery [Tuncer and Kocuk, 2023]. Benders decomposition separates unit commitment decisions from network feasibility checks, but they often suffer from slow convergence and require careful tuning of cuts and coordination between subproblems [Tuncer and Kocuk, 2023].

The second class is the outer approximation (OA) methods. OA focuses on constructing a linear relaxation to either the nonlinear objective function in UC [Ruiz et al., 2013] or the nonlinear constraints [Castillo et al., 2016, Liu et al., 2018], then iteratively solves the LP or MILP and tightens the relaxation based on the suboptimal or infeasible solution. However, OA methods suffer from slow convergence and no detected feasible solution before termination. A potential enhanced strategy is the outer-inner approximation method [Han et al., 2013], which adopts an inner approximation to find a feasible solution earlier. However,

in AC-UC, finding a feasible solution for MINLP is naturally NP-hard.

Another popular class is using DC power flow approximations, which have become the industry standard due to advances in solver technology and strong formulations [Ostrowski et al., 2011, Knueven et al., 2020]. These methods can solve large-scale UC problems efficiently, but they neglect reactive power and voltage constraints, which may lead to infeasibility. Even though AC corrective actions or redispatching can be used to recover the solution, it may cause a prominent optimality gap [Parker and Coffrin, 2024].

In this paper, we focus on the SOC relaxation for UC, which is proposed in [Bai et al., 2015, Liu et al., 2018]. While the relaxation convexifies the continuous network laws with SOCs, commitment decisions need to be made, resulting in an MISOCP, which is computationally challenging due to the high cost and low numerical robustness of solving conic subproblems within the branch-and-bound framework. To mitigate these issues, some authors have proposed strengthening the SOCP relaxation using valid inequalities and bound tightening [Kocuk et al., 2016, Coffrin et al., 2015], as well as decomposition algorithms to separate commitment decisions and AC feasibility [Bai et al., 2015, Constante-Flores et al., 2022, Tuncer and Kocuk, 2023].

Despite being substantially harder to solve than the DC unit commitment problem formulated as a mixed-integer linear program [Carrión and Arroyo, 2006, Conejo and Baringo, 2018], SOC-relaxed AC-UC provides commitments that are more consistent with physical network constraints. SOC-based AC-UC captures key AC feasibility aspects while maintaining convexity in the continuous relaxation, producing tighter lower bounds and more reliable commitment decisions even if the relaxation is not exact [Jabr, 2006]. Furthermore, the MISOCP relaxations are computationally more tractable than MISDP relaxations [Coffrin et al., 2016]. As a result, SOC-based AC unit commitment is widely viewed as a principled compromise between the scalability of DC unit commitment and the accuracy of full nonconvex AC-UC [Tuncer and Kocuk, 2023].

Motivated by these challenges, we propose a progressive integrality outer–inner approximation framework for solving SOC-based AC network-constrained unit commitment (NCUC) problems efficiently. The key idea is to decouple the treatment of nonlinear constraints and integrality. Specifically, we construct an outer approximation that provides valid lower bounds via MILPs, and an inner approximation generating feasible solutions by solving convex SOCPs with fixed commitments. To further improve computational efficiency, we introduce a progressive integrality strategy that gradually enforces integrality, starting from LP relaxation and moving toward full MILP. This allows the algorithm to generate strong cuts at low cost in early iterations while focusing computational effort on integrality only when necessary. In addition, we incorporate time-block Benders cuts that leverage dual information from the inner problem to strengthen the outer approximation and accelerate convergence.

1.1 Contribution and Organization

Our contributions are:

(1) We develop an outer–inner approximation framework for SOC-based AC NCUC that alternates between MILP-based relaxation and SOCP-based feasible solution detection, enabling simultaneous improvement of lower and upper bounds.

(2) We propose a progressive integrality strategy that significantly reduces computational effort by gradually enforcing integrality, improving scalability for large-scale instances.

(3) We introduce time-block Benders cuts that strengthen the relaxation using dual information from the inner problem, leading to faster convergence.

(4) We demonstrate the effectiveness and robustness of the proposed framework on large-scale test systems, including 200-bus and 500-bus networks, under different formulations and perturbed load scenarios.

We note that the idea to solve such SOC-based AC NCUC by outer approximation with cuts proposed by Bienstock and Villagra [2025] first appeared in [Dai et al., 2025]. This work significantly extends the outer approximation in three approaches:

(1) The outer approximation in [Dai et al., 2025, Dai and Conjeo, 2026] is a subroutine of Column-and-Constraint generation or Benders decomposition, while in this work, we develop an independent method for AC-UC.

(2) The method developed in Section 3.2 adopts dynamic MIP gaps, dynamic MIP time limits, and warm start in MILP solutions, which significantly reduces the overall solution time.

(3) The progressive integrality framework in Section 3.3 and time-block Benders cuts in Section 3.4 are new, which further improve the speed and scalability of the method.

The remainder of this paper is organized as follows. Section 2 presents the SOC-ACUC formulation. Section 3 describes the proposed solution methodology. Section 4 reports numerical experiments. Section 5 concludes the paper.

2 Formulation

2.1 Model Formulation

We detail the formulation of the SOC-relaxed AC NCUC problem in this section. For convenience, we call the problem SOC-NCUC.

2.1.1 Objective function: minimize expected cost

The objective function (1) contains the startup, shutdown, and operation costs of all the units, and penalties for unserved demands and over-produced power.

$$\min_{u,y,z,p,q} \sum_{t\in\mathcal{T}}\sum_{g\in\mathcal{G}}(C_g^{\mathrm{F}}u_{g,t} + C_g^{\mathrm{SU}}y_{g,t} + C_g^{\mathrm{SD}}z_{g,t} + C_g^{\mathrm{V}}p_{g,t}) \tag{1a}$$

$$+\sum_{t\in\mathcal{T}}\sum_{n\in\mathcal{N}} C^{\mathrm{P}}(p_{n,t}^{\mathrm{U}} + q_{n,t}^{\mathrm{U}}) \tag{1b}$$

$$+\sum_{t\in\mathcal{T}}\sum_{n\in\mathcal{N}} C^{\mathrm{P}}(p_{n,t}^{\mathrm{O}} + q_{n,t}^{\mathrm{O}}) \tag{1c}$$

The function (1a) is the most standard objective for unit commitment. In robust optimization, e.g., [Constante-Flores et al., 2022, Constante-Flores and Conejo, 2024], we also consider unserved demands/power shedding, as (1b), and over-generation/surplus generation, as (1c), to guarantee the feasibility of the unit commitment model. Both power shedding and surplus generation potentially threaten the safety of the power network; thus, we should give a high penalty cost C^{P}.

2.1.2 Constraints for commitment variables

$$y_{g,t} - z_{g,t} = u_{g,t} - u_{g,t-1}, \quad \forall t = 2, ..., T, \forall g \in \mathcal{G} \tag{2a}$$

$$y_{g,1} - z_{g,1} = u_{g,1} - u_{g,0}, \quad \forall g \in \mathcal{G} \tag{2b}$$

$$y_{g,t} + z_{g,t} \leq 1, \quad \forall t \in \mathcal{T}, \forall g \in \mathcal{G} \tag{2c}$$

$$u_{g,t}, y_{g,t}, z_{g,t} \in \{0, 1\}, \quad \forall t = 2, ..., T, \forall g \in \mathcal{G} \tag{2d}$$

$$\sum_{t=1}^{L_g}(1 - u_{g,t}) = 0, \quad \forall g \in \mathcal{G}^{\mathrm{T}} \tag{2e}$$

$$\sum_{t=\tilde{t}}^{\tilde{t}+T_g^{\mathrm{U}}-1} u_{g,t} \geq T_g^{\mathrm{U}} y_{g,\tilde{t}}, \quad \forall \tilde{t} = L_g + 1, ..., T - T_g^{\mathrm{U}} + 1, \forall g \in \mathcal{G}^{\mathrm{T}} \tag{2f}$$

$$\sum_{t=\tilde{t}}^{\mathrm{T}}(u_{g,t} - y_{g,t}) \geq 0, \quad \forall \tilde{t} = T - T_g^{\mathrm{U}} + 2, ..., T, \forall g \in \mathcal{G}^{\mathrm{T}} \tag{2g}$$

$$\sum_{t=1}^{F_g} u_{g,t} = 0, \quad \forall g \in \mathcal{G}^{\mathrm{T}} \tag{2h}$$

$$\sum_{t=\tilde{t}}^{t_i+T_g^{\mathrm{D}}-1} (1 - u_{g,t}) \geq T_g^{\mathrm{D}} z_{g,\tilde{t}}, \quad \forall \tilde{t} = F_g + 1, ..., T - T_g^{\mathrm{D}} + 1, \forall g \in \mathcal{G}^{\mathrm{T}} \tag{2i}$$

$$\sum_{t=\tilde{t}}^{\mathrm{T}}(1 - u_{g,t} - z_{g,t}) \geq 0, \quad \forall \tilde{t} = T - T_g^{\mathrm{D}} + 2, ..., T, \forall g \in \mathcal{G}^{\mathrm{T}} \tag{2j}$$

Logic constraints Constraints (2a)-(2d) are logic constraints for units' startup, shutdown, and on/off status variables. Specifically, (2a) enforces a startup

($y_{g,t} = 1$) if the generating unit transitions from off to on, and a shutdown ($z_{g,t} = 1$) if the generating unit transitions from on to off. (2b) is for the first time period, where $u_{g,0}$ is a constant. (2c) ensures a unit does not start up and shut down in the same time.

Minimum up/down constraints Minimum up and down times of thermal units are enforced by constraints (2e)-(2j). We note that if a thermal generating unit $g \in \mathcal{G}^{\mathrm{T}}$ starts up or shuts down, it needs to be keep on/off during the minimum up/down time $T_g^{\mathrm{U}}/T_g^{\mathrm{D}}$. Additionally, the unit g is required to be on/off during the first L_g/F_g periods based on its initial status in $t = 0$. Also, we have $L_g \cdot F_g = 0$ to prevent a unit to be up and down at the same time. (2e)/(2h) enforces that unit g remains on/off during the initial up/down time. (2f)/(2i) ensures that unit g remains on/off during the minimum up/down time after a startup/shutdown. When the required up/down time exceeds the total planning time range, (2g)/(2j) enforces that unit g remains on/off until the last period T.

2.1.3 Constraints for active and reactive power output

$$p_g^{\min} u_{g,t} \leq p_{g,t} \leq p_g^{\max} u_{g,t}, \quad \forall t \in \mathcal{T}, g \in \mathcal{G} \tag{3a}$$

$$p_{g,t} \leq \bar{p}_{g,t} \leq p_g^{\max} u_{g,t}, \quad \forall t \in \mathcal{T}, g \in \mathcal{G} \tag{3b}$$

$$q_g^{\min} u_{g,t} \leq q_{g,t} \leq q_g^{\max} u_{g,t}, \quad \forall t \in \mathcal{T}, g \in \mathcal{G} \tag{3c}$$

$$p_{g,t} - p_{g,t-1} \leq R_g^{\mathrm{U}} u_{g,t-1} + R_g^{\mathrm{SU}} y_{g,t}, \quad \forall t \in \mathcal{T}, g \in \mathcal{G}^{\mathrm{T}} \tag{3d}$$

$$\bar{p}_{g,t} \leq p_{g,t-1} + R_g^{\mathrm{U}} u_{g,t-1} + R_g^{\mathrm{SU}} y_{g,t}, \quad t \in \mathcal{T}, g \in \mathcal{G}^{\mathrm{T}} \tag{3e}$$

$$p_{g,t-1} - p_{g,t} \leq R_g^{\mathrm{D}} u_{g,t-1} + R_g^{\mathrm{SD}} z_{g,t}, \quad \forall t \in \mathcal{T}, g \in \mathcal{G}^{\mathrm{T}} \tag{3f}$$

$$\bar{p}_{g,t} \leq p_g^{\max}(u_{g,t} - z_{g,t+1}) + z_{g,t+1} R_g^{\mathrm{SD}}, \quad \forall t \in \mathcal{T}, g \in \mathcal{G}^{\mathrm{T}} \tag{3g}$$

$$\sum_{g \in \Omega_r} \bar{p}_{g,t} - p_{g,t} \geq R_{r,t}^{\mathrm{D}}, \quad \forall g \in \mathcal{G}^{\mathrm{T}}, \forall r \in \mathcal{R} \tag{3h}$$

Range for power outputs The actual power output of each unit has a lower bound as its minimum power output and an upper bound as its maximum available power by constraints (3a)-(3c). We also include the maximum available power $\bar{p}_{g,t}$ of unit g in period t, which depends on the ramping limit and is needed to meet a reserve requirement per area (see Constraint (3h)), and that is upper bounded by the active power capacity of the unit.

Ramping Limits Constraints (3d)-(3g) impose the ramping limit to both the generation level $p_{g,t}$ and its upper bound $\bar{p}_{g,t}$. Specifically, (3d)/(3e) is the up and startup ramping limit for $p_{g,t}/\bar{p}_{g,t}$, while (3f)/(3g) are for the down and shutdown ramping limit.

Area reserve requirement For each reserve area $r \in \mathcal{R}$, we enforce that the maximum available active power output $\bar{p}_{g,t}$ and the active power produced $p_{g,t}$ satisfy some pre-specified reserve requirements, which are set by constraints (3h).

2.1.4 Constraints for power flow and network

$$p_{n,m,t} = -G_{n,m}c_{n,n,t} + G_{n,m}c_{n,m,t} - B_{n,m}s_{n,m,t}, \quad \forall t \in \mathcal{T}, \forall (n,m) \in \mathcal{E} \tag{4a}$$

$$q_{n,m,t} = (B_{n,m} - b^{\text{shunt}}_{n,m})c_{n,n,t} - G_{n,m}s_{n,m,t} - B_{n,m}c_{n,m,t}, \quad \forall t \in \mathcal{T}, \forall (n,m) \in \mathcal{E} \tag{4b}$$

$$c_{n,m,t} = c_{m,n,t}, s_{n,m,t} = -s_{m,n,t}, \quad \forall t \in \mathcal{T}, \forall (n,m) \in \mathcal{E} \tag{4c}$$

$$c^2_{n,m,t} + s^2_{n,m,t} \leq c_{n,n,t}c_{m,m,t}, \quad \forall t \in \mathcal{T}, \forall (n,m) \in \mathcal{E} \tag{4d}$$

$$-V^{\max}_n V^{\max}_m \leq c_{n,m,t} \leq V^{\max}_n V^{\max}_m, \quad \forall t \in \mathcal{T}, \forall (n,m) \in \mathcal{E} \tag{4e}$$

$$-V^{\max}_n V^{\max}_m \leq s_{n,m,t} \leq V^{\max}_n V^{\max}_m, \quad \forall t \in \mathcal{T}, \forall (n,m) \in \mathcal{E} \tag{4f}$$

$$V^{\min 2}_n \leq c_{n,n,t} \leq V^{\max 2}_n, \quad \forall t \in \mathcal{T}, \forall (n,m) \in \mathcal{E} \tag{4g}$$

Constraints (4a), (4b), (4c), and (4d) are the power flow equations with second-order-conic relaxation [Jabr, 2006]. The details for the formulation can be found in, e.g., [Kocuk et al., 2016, Constante-Flores et al., 2022, Bienstock and Villagra, 2025]. Here we provide a simple description.

The complex voltage for a node n at period t is in the polar form, $V_{n,t} = |V_{n,t}|(\cos\theta_{n,t} + \mathrm{i}\sin\theta_{n,t})$, where $\theta_{n,t}$ is the voltage magnitude in bus n at time t. For a line (n,m), let $c_{n,n,t} := V^2_{n,t} \in [V^{\min 2}_n, V^{\max 2}_n]$ (bounds in (4e)), $c_{n,m,t} := |V_{n,t}||V_{m,t}|\cos(\theta_{n,m,t}) \in [-V^{\max}_n V^{\max}_m, V^{\max}_n V^{\max}_m]$ (bounds in (4f)), and $s_{n,m,t} := -|V_{n,t}||V_{m,t}|\sin(\theta_{n,m,t}) \in [-V^{\max}_n V^{\max}_m, V^{\max}_n V^{\max}_m]$ bounds in (4g)). Then, considering [Kocuk et al., 2017, (1), (4d),(4e)], we have (4a) and (4b) as the active and reactive power flow based on $c_{n,n,t}, c_{n,m,t}, s_{n,m,t}$. Also, (4c) are properties for $c_{n,n,t}, c_{n,m,t}, s_{n,m,t}$, see [Kocuk et al., 2017, (4f)].

We also note that $c^2_{n,m,t} + s^2_{n,m,t} = c_{n,n,t}c_{m,m,t}$ is a nonconvex quadratic constraint. We relax this constraint as $c^2_{n,m,t} + s^2_{n,m,t} \leq c_{n,n,t}c_{m,m,t}$ as (4d), which is a second-order cone constraint.

2.1.5 Constraints for power flows

The active and reactive power balances involving power generations, demands, unserved demands, over-produced power, and power flows are ensured by constraints (5a) and (5b), respectively.

$$\sum_{g \in \Lambda^{\text{G}}_n} p_{g,t} - p^{\text{D}}_{n,t} + p^{\text{U}}_{n,t} - p^{\text{O}}_{n,t} = \sum_{m \in \Lambda_n} p_{n,m,t}, \quad \forall t \in \mathcal{T}, n \in \mathcal{N} \tag{5a}$$

$$\sum_{g \in \Lambda^{\text{G}}_n} q_{g,t} - q^{\text{D}}_{n,t} + q^{\text{U}}_{n,t} - q^{\text{O}}_{n,t} = \sum_{m \in \Lambda_n} q_{n,m,t}, \quad \forall t \in \mathcal{T}, n \in \mathcal{N} \tag{5b}$$

$$p_{n,m,t}^2 + q_{n,m,t}^2 \leq S_{n,m,t}^2, \quad \forall t \in \mathcal{T}, \forall (n,m) \in \mathcal{E} \tag{5c}$$
$$0 \leq p_{n,t}^{\mathrm{U}} \leq p_{n,t}^{\mathrm{D}}, \quad \forall n \in \mathcal{N}, t \in \mathcal{T} \tag{5d}$$
$$0 \leq q_{n,t}^{\mathrm{U}} \leq q_{n,t}^{\mathrm{D}}, \quad \forall n \in \mathcal{N}, t \in \mathcal{T} \tag{5e}$$
$$p_{n,t}^{\mathrm{O}}, q_{n,t}^{\mathrm{O}} \geq 0, \quad \forall n \in \mathcal{N}, t \in \mathcal{T} \tag{5f}$$

Active and reactive power balance The active and reactive power balances involving power generations, demands, unserved demands, over-produced power, and power flows are ensured by constraints (5a) and (5b), respectively.

Line capacity limit Constraints (5c), which are quadratic constraints, force the transmission capacity limits.

Bounds for slack variables Slack variables $p_{n,t}^{\mathrm{U}}, q_{n,t}^{\mathrm{U}}$ are bounded by constraints (5d) and (5e), while $p_{n,t}^{\mathrm{O}}, q_{n,t}^{\mathrm{O}}$ are non-negative by constraints (5f).

2.2 Compact formulation

For convenience in later algorithm description, we compactly write SOC-NCUC:

$$\mathcal{M} := \min \ c_x^T \boldsymbol{x} + c_y^T \boldsymbol{y} + c_z^T \boldsymbol{z} \tag{6a}$$
$$\text{s.t. } A\boldsymbol{x} \leq b \tag{6b}$$
$$E\boldsymbol{x} + F\boldsymbol{y} + G\boldsymbol{z} \leq d \tag{6c}$$
$$\boldsymbol{g}^{\mathrm{soc}}(\boldsymbol{z}) \leq 0 \tag{6d}$$
$$\boldsymbol{g}^{\mathrm{cap}}(\boldsymbol{z}) \leq 0 \tag{6e}$$
$$\boldsymbol{x} \in \{0,1\}^{|\boldsymbol{x}|}. \tag{6f}$$

The variable $\boldsymbol{x}$ contains all commitment variables, i.e., $u_{g,t}, y_{g,t}, z_{g,t}$, the variable $\boldsymbol{y}$ contains all dispatch variables, e.g., $p_{g,t}, \bar{p}_{g,t}, q_{g,t}$, the variable $\boldsymbol{z}$ contains all network variables, e.g., $p_{n,m,t}, q_{n,m,t}, c_{n,m,t}, s_{n,m,t}, c_{n,n,t}$ and slack variables $p_{n,t}^U, q_{n,t}^U, p_{n,t}^O, q_{n,t}^O$.

In the objective function (6a), c_x contains the cost for commitment operations, c_y contains the variable cost of generators, and c_z contains the penalty cost for slack variables.

Constraint (6b) includes linear constraints that only contain commitment variables, i.e., (2). Constraint (6c) represents all other linear constraints. We use $\boldsymbol{g}^{\mathrm{cap}}(\cdot)$ and $\boldsymbol{g}^{\mathrm{soc}}(\cdot)$ to represents nonlinear functions in line capacity limit (5c), i.e., $p_{n,m,t}^2 + q_{n,m,t}^2 - S_{n,m,t}^2$, and second-order cone constraint (4d), i.e., $c_{n,m,t}^2 + s_{n,m,t}^2 - c_{n,n,t} c_{m,m,t}$, separately.

3 Progressive Integrality Outer–Inner Approximation Framework

3.1 Overview of the Proposed Framework

SOC-NCUC is an MISOCP, which is computationally challenging to solve directly [Bonami et al., 2011]. To address this, we propose a progressive integrality outer–inner approximation (PIOIA) framework. The key idea is to separate nonlinear constraints and integrality, handling them through alternating approximations and progressively enforcing integrality.

The proposed framework consists of three stages: (1) a linear programming relaxation stage to construct strong cuts efficiently, (2) a progressive integrality stage to enforce integrality progressively, and (3) a full outer–inner approximation stage to close the optimality gap. Finally, we introduce time-block Benders cuts to accelerate convergence.

3.2 Outer–Inner Approximation Backbone

We decompose SOC-NCUC into two complementary approximations: (1) an outer approximation, i.e., an MINLP, which drops nonlinear constraints from SOC-NCUC and adds some linear cuts; (2) an inner approximation, i.e., a SOCP, which fixes binary variables by a given solution, typically from the outer approximation. Then we develop the alternating outer-inner approximate method to find a (near-)optimal solution for SOC-NCUC. Unlike classical outer approximation methods that only strengthen the relaxation, the proposed method alternates between outer and inner approximations to simultaneously improve lower and upper bounds.

3.2.1 Outer and Inner Approximations

There are two nonlinear constraints in SOC-NCUC: the quadratic line capacity constraint (5c) or (6e), and the second-order cone constraint (4d) or (6d). To approximate nonlinear constraints, we construct supporting hyperplanes at violated points, leading to the following linear cuts proposed by Bienstock and Villagra [2025]:

(1) Regarding the line capacity constraint $p_{n,m,t}^2 + q_{n,m,t}^2 \leq S_{n,m}^2$, if a solution $(\bar{p}_{n,m,t}, \bar{q}_{n,m,t})$ violates this constraint, we add the linear cut

$$\bar{p}_{n,m,t} p_{n,m,t} + \bar{q}_{n,m,t} q_{n,m,t} \leq S_{n,m} \|(\bar{p}_{n,m,t}, \bar{q}_{n,m,t})\|_2; \tag{7}$$

(2) Regarding the second-order cone constraint $c_{n,m,t}^2 + s_{n,m,t}^2 \leq c_{n,n,t} c_{m,m,t}$, if a solution $(\bar{c}_{n,m,t}, \bar{s}_{n,m,t}, \bar{c}_{n,n,t}, \bar{c}_{m,m,t})$ violates this constraint, we add the cut

$$\begin{aligned} &4\bar{c}_{n,m,t} c_{n,m,t} + 4\bar{s}_{n,m,t} s_{n,m,t} + (\bar{c}_{n,n,t} - \bar{c}_{m,m,t} - n_0) c_{n,n,t} \\ &- (\bar{c}_{n,n,t} - \bar{c}_{m,m,t} + n_0) c_{m,m,t} \leq 0, \end{aligned} \tag{8}$$

where $n_0 = \|2\bar{c}_{n,m,t}, 2\bar{s}_{n,m,t}, \bar{c}_{n,n,t}, \bar{c}_{m,m,t}\|_2$.

We use $\mathcal{K}^{\text{cap}}$ and $\mathcal{K}^{\text{soc}}$ to cache all generated cuts (7) and (8) separately. Then we drop nonlinear constraints (6d) and (6e) from the original MISOCP (6) and add linear cuts from set $\mathcal{K}^{\text{soc}}$ and $\mathcal{K}^{\text{cap}}$ to construct the outer approximation for SOC-NCUC as follows.

$$\begin{aligned}
\mathcal{O}(\mathcal{K}^{\text{soc}}, \mathcal{K}^{\text{cap}}) := \min\ & c_x^T \boldsymbol{x} + c_y^T \boldsymbol{y} + c_z^T \boldsymbol{z} && \text{(9a)}\\
\text{s.t. } & (6b), (6c) \\
& a_z^{\text{soc}} \boldsymbol{z} \le 0, \forall a_z^s \in \mathcal{K}^{\text{soc}} && \text{(9b)}\\
& a_z^{\text{cap}} \boldsymbol{z} \le 0, \forall a_z^c \in \mathcal{K}^{\text{cap}} && \text{(9c)}\\
& \boldsymbol{x} \in \{0,1\}^{|\boldsymbol{x}|}. && \text{(9d)}
\end{aligned}$$

Given any solution $\boldsymbol{x}'$ satisfying (6b), then we can fix $\boldsymbol{x} = \boldsymbol{x}'$ in the original MISOCP (6) to get an inner approximation:

$$\begin{aligned}
\mathcal{I}(\boldsymbol{x}') := \min\ & c_x^T \boldsymbol{x} + c_y^T \boldsymbol{y} + c_z^T \boldsymbol{z} && \text{(10a)}\\
\text{s.t. } & (6b), (6c), (6d), (6e), \\
& \boldsymbol{x} = \boldsymbol{x}'. && \text{(10b)}
\end{aligned}$$

The inner approximation $\mathcal{I}(\boldsymbol{x}')$ is a convex SOCP, which is polynomial solvable to any desired accuracy.

3.2.2 Alternating Outer-Inner Approximate Method

Solving the outer approximation $\mathcal{O}(\mathcal{K}^{\text{soc}}, \mathcal{K}^{\text{cap}})$ can provide us with a valid lower bound (LB) and a $\boldsymbol{x}$ which satisfies constraint (2). Hence, we can get an inner approximation $\mathcal{I}(\boldsymbol{x})$, whose feasible solution is also feasible to the original SOC-NCUC, i.e., providing a valid UB. Therefore, we can alternatively solve $\mathcal{O}(\mathcal{K}^{\text{soc}}, \mathcal{K}^{\text{cap}})$ and $\mathcal{I}(\boldsymbol{x}')$ to find a (near-)optimal solution for $\mathcal{M}$ with a desired convergence tolerance as Algorithm 1.

We note that, in the algorithm, $\boldsymbol{x}, \boldsymbol{y}, \boldsymbol{z}$ are solutions from the outer approximation $\mathcal{O}(\mathcal{K}^{\text{soc}}, \mathcal{K}^{\text{cap}})$, and $\boldsymbol{y}', \boldsymbol{z}'$ are solutions from the inner approximation $\mathcal{I}(\boldsymbol{x})$.

In lines 2 and 13, we solve MILPs with a pre-set MIP gap δ_{mip}, which implies the solver will stop once it closes the MIP gap less than or equal to δ_{mip}, and a time limit t_{solver}, which is the maximum runtime of the solver. In earlier iterations, it is unnecessary to solve all MILPs to optimality, as this is time-consuming and ineffective. Also, we will feed a feasible solution to the MIP solver in line 13 as a warm start.

In line 5, the ϵ_{tol}-active constraint implies $\boldsymbol{g}^{\text{cap}}(\boldsymbol{z}') \ge -\epsilon_{\text{tol}}$. We adopt an active-set strategy that only considers binding line capacity constraints based on the solution of the inner problem, because most line capacity constraints are not active in the optimal solution [Bienstock and Villagra, 2025]. Such an active-set strategy can reduce the number of added cuts and reduce the solution time.

Algorithm 1: Alternating Outer-Inner Approximate Method

Input: ϵ, ϵ_{tol}, p_{cut}, ϵ_{par}, δ_{mip}, max_iter, and t_{solver}.
Output: $\boldsymbol{x}$ and obj

1 Initialize $\mathcal{K}^{\text{soc}} = \emptyset$, $\mathcal{K}^{\text{cap}} = \emptyset$, UB $:= +\infty$;
2 Set LB be the dual bound by solving $\mathcal{O}(\mathcal{K}^{\text{soc}}, \mathcal{K}^{\text{cap}})$ with the pre-set MIP gap δ_{mip} and the time limit t_{solver}, and get $\boldsymbol{x}, \boldsymbol{y}, \boldsymbol{z}$;
3 **while** $\frac{\text{UB}-\text{LB}}{\text{UB}} > \epsilon$ **do**
4 Set obj* be the optimal value by solving $\mathcal{I}(\boldsymbol{x})$, and get $\boldsymbol{y}', \boldsymbol{z}'$.;
5 Set UB $:= \min\{\text{obj}^*, \text{UB}\}$ and check for active $\boldsymbol{g}^{\text{cap}}(\boldsymbol{z}') \leq 0$;
6 Check for ϵ_{tol}-violated $\boldsymbol{g}^{\text{soc}}(\boldsymbol{z}) \leq 0$ for all inequalities and $\boldsymbol{g}^{\text{cap}}(\boldsymbol{z}') \leq 0$ only for active inequalities;
7 Generate cuts for p_{cut} most violated inequalities;
8 Add the cut to $\mathcal{K}^{\text{soc}}$ or $\mathcal{K}^{\text{cap}}$ if it is not ϵ_{par}-parallel to added cuts;
9 Set $\delta_{\text{mip}} := \min\{0.9 \times \delta_{\text{mip}}, \frac{\text{UB}-\text{LB}}{4\text{UB}}\}$, and $t_{\text{solver}} := 1.1 \times t_{\text{solver}}$;
10 Set LB be the dual bound by solving $\mathcal{O}(\mathcal{K}^{\text{soc}}, \mathcal{K}^{\text{cap}})$ with the pre-set MIP gap δ_{mip} and the time limit t_{solver}, and $\boldsymbol{x}, \boldsymbol{y}, \boldsymbol{z}$ be the solution;
11 **end**
12 **return** $\boldsymbol{x}$, UB.

In line 6, the ϵ_{tol}-violated constraint implies $\boldsymbol{g}(\boldsymbol{z}) > \epsilon_{\text{tol}}$.

In line 8, we note that two cuts, e.g., $c_1^T x \leq 0$ and $c_2^T x \leq 0$, are not ϵ_{par}-parallel when the cosine of the angle formed by $c_1/\|c_1\|$ and $c_2/\|c_2 2\|$ is less than or equal to $1 - \epsilon_{\text{par}}$. We reject "too parallel" cuts to avoid numerical issues in solving MILPs [Higham, 2002, Klotz, 2014].

This alternating scheme differs from standard outer approximation for MINLP, where only LB is improved, and from Benders-type methods, where feasibility is enforced via cuts without solving a nonlinear subproblem.

3.3 Progressive Integrality Strategy

Although the outer–inner framework improves solution quality, solving full MILPs in each iteration remains computationally expensive. This motivates the progressive integrality strategy proposed in this section. More specifically, we progressively enforce integrality through three stages: (1) linear programming relaxation, (2) integrality generation, and (3) full integrality. We begin by solving the linear programming (LP) relaxation to $\mathcal{O}(\mathcal{K}^{\text{soc}}, \mathcal{K}^{\text{cap}})$ in earlier iterations, and then we continue selecting part of $\boldsymbol{x}$ to be binary and solve the partial-integrality relaxation to $\mathcal{O}(\mathcal{K}^{\text{soc}}, \mathcal{K}^{\text{cap}})$. Finally, we set all $\boldsymbol{x}$ variables to binary and solve the fully MILP with the proposed time-block Benders cuts in later iterations.

For convenience, we drop (9*d*) and construct a relaxation to $\mathcal{O}(\mathcal{K}^{\text{soc}}, \mathcal{K}^{\text{cap}})$

with a index set $\mathcal{B}$:

$$\begin{aligned}\bar{\mathcal{O}}(\mathcal{K}^{\text{soc}}, \mathcal{K}^{\text{cap}}, \mathcal{B}) := \min\{c_x^T \boldsymbol{x} + c_y^T \boldsymbol{y} + c_z^T \boldsymbol{z} : \\ (6b), (6c), (9b), (9c), \\ \boldsymbol{x}_i \in \{0,1\}, \forall i \in \mathcal{B}\}.\end{aligned} \tag{11}$$

If $\mathcal{B} := \emptyset$, then $\bar{\mathcal{O}}(\mathcal{K}^{\text{soc}}, \mathcal{K}^{\text{cap}}, \mathcal{B}\})$ is the LP relaxation. If $\mathcal{B} := \{1, ..., |\boldsymbol{x}|\}$, i.e., all indexes of $\boldsymbol{x}$, then $\bar{\mathcal{O}}(\mathcal{K}^{\text{soc}}, \mathcal{K}^{\text{cap}}, \mathcal{B}\}) = \mathcal{O}(\mathcal{K}^{\text{soc}}, \mathcal{K}^{\text{cap}})$.

3.3.1 Linear Programming Stage

From the literature of branch-and-bound for MINLP, see e.g., [Quesada and Grossmann, 1992, Bonami et al., 2008, Kronqvist et al., 2019, Bestuzheva et al., 2025], we observe that, in the root node, solvers usually focus on constructing a linear relaxation for the continuous relaxation of MINLP. Therefore, we develop an LP stage as Algorithm 2.

Algorithm 2: Linear Programming Stage

Input: ϵ_{tol}, p_{cut}, ϵ_{par}, max_iter, and ϵ_{LP}.
Output: $\mathcal{K}^{\text{soc}}, \boldsymbol{x}$ and LB

1 Initialize $\mathcal{K}^{\text{soc}} = \emptyset$, $\text{LB}_{\text{old}} = 0$;
2 Set LB be the objective value of $\bar{\mathcal{O}}(\mathcal{K}^{\text{soc}}, \emptyset, \emptyset)$, and $\boldsymbol{x}, \boldsymbol{y}, \boldsymbol{z}$ be the solution;
3 **while** $\frac{\text{LB}_{\text{old}} - \text{LB}}{\text{LB}} > \epsilon_{\text{LP}}$ **do**
4 Check for ϵ_{tol}-violated $\boldsymbol{g}^{\text{soc}}(\boldsymbol{z}) \leq 0$ for all inequalities;
5 Generate cuts for p_{cut} most violated inequalities;
6 Add the cut to $\mathcal{K}^{\text{soc}}$ if it is not ϵ_{par}-parallel to added cuts;
7 Set $\text{LB}_{\text{old}} := \text{LB}$;
8 Set LB be the objective value of $\bar{\mathcal{O}}(\mathcal{K}^{\text{soc}}, \emptyset, \emptyset)$, and get $\boldsymbol{x}, \boldsymbol{y}, \boldsymbol{z}$;
9 **end**
10 **return** $\mathcal{K}^{\text{soc}}, \boldsymbol{x}$ and LB.

Because solving the LP relaxation cannot provide an integrality-feasible $\boldsymbol{x}$, we do not solve $\mathcal{I}(\boldsymbol{x})$; thus, the LP stage cannot provide a valid UB for the original SOC-NCUC, as well as the active-set strategy for $\boldsymbol{g}^{\text{cap}}(\cdot) \leq 0$. Therefore, we focus on finding a valid (and hopefully good) LB and constructing a linear relaxation for $\boldsymbol{g}^{\text{soc}}(\cdot) \leq 0$ in the LP stage.

In line 9 of Algorithm 2, the LP stage will terminate if the improvement rate of the LB in two iterations is less than a pre-set ϵ_{LP}.

Remark 1. Let $\mathcal{F}(P)$ be the feasible region of the problem P, and obj(P) be the optimal value of P. We note that:

(1) SOC cuts valid for the continuous relaxation to $\mathcal{M}$ are also valid for $\mathcal{M}$, because $\mathcal{F}(\mathcal{M}) \subseteq \mathcal{F}$(Continuous Relaxation of $\mathcal{M}$).

(2) Cuts of $\mathcal{K}^{\text{SOC}}$ from Algorithm 2 are valid for $\mathcal{M}$, because of (1).

(3) The LB from Algorithm 2 are valid for $\mathcal{M}$, i.e., LB $\leq$ obj($\mathcal{M}$), because LB $\leq$ obj($\bar{\mathcal{O}}(\mathcal{K}^{\text{soc}}, \emptyset, \emptyset)$) $\leq$ obj(Continuous Relaxation of $\mathcal{M}$) $\leq$ obj($\mathcal{M}$).

The main advantage of Algorithm 2 is that it provides a valid LB and a linear relaxation to SOC-NCUC via solving some LPs, which is far computationally cheaper than solving the same number of MIPs. Therefore, deploying the LP stage before Algorithm 1 may reduce the number of MILPs to solve, and hence, bring a significant computational benefit.

3.3.2 Integrality Generation Stage

The LP stage improves the LB efficiently because it solves LPs rather than MILPs. However, as the LB approaches the optimal value of the continuous relaxation of $\mathcal{M}$, further improvements may stall or become very slow, even though a non-negligible gap to the optimal value of the original $\mathcal{M}$ remains. To address this issue, we propose a transition stage between Algorithm 2 and Algorithm 1, which aims to (1) further improve the lower bound and strengthen the linear relaxation, and (2) avoid solving the full MILP $\mathcal{O}(\mathcal{K}^{\text{soc}}, \mathcal{K}^{\text{cap}})$ "too early". In the transition stage, we pick some variables and set them as binaries, i.e., the partial MILP, which we call *integrality generation*. This strategy balances exploration (LP relaxation) and exploitation (integrality), similar to progressive refinement in branch-and-bound.

After solving $\bar{\mathcal{O}}(\mathcal{K}^{\text{soc}}, \emptyset, \mathcal{B})$, we have the optimal solution $\boldsymbol{x}^*$. The solution $\boldsymbol{x}^*(g,t)$ represents the corresponding unit commitment variables $(u^*_{g,t}, y^*_{g,t}, z^*_{g,t})$. For each generator $g \in \mathcal{G}$, we compute

$$\text{score}_g := \sum_{t \in \mathcal{T}} \min\{u^*_{g,t}, 1 - u^*_{g_t}\}. \tag{12}$$

This score aggregates the degree of fractionalness across all time periods, favoring generators whose commitment decisions are consistently fractional. Such variables are more likely to impact the LB and are therefore prioritized for binary enforcement.

We select (at most) k generators with the largest scores, and set $u_{g,t}, y_{g,t}, z_{g,t}$ for picked generators g and all $t \in \mathcal{T}$ as binary variables, i.e., $\boldsymbol{x}(g,t) \in \{0,1\}^3$ and $\mathcal{B} := \mathcal{B} \cup \{\boldsymbol{x}(g,t)\}$.

We develop an *Integrality Generation Stage* (IG stage) as Algorithm 3. We do not solve $\mathcal{I}(\boldsymbol{x})$ for UB again due to the same reason in the LP stage that $\boldsymbol{x}$ is not integrality-feasible. In line 7, the IG stage will terminate if the improvement rate of LB between two continuous iterations is less than ϵ_{IG} or all $\boldsymbol{x}$ have been set as binary variables.

Remark 2. The lower bound and cuts generated from $\bar{\mathcal{O}}(\mathcal{K}^{\text{soc}}, \emptyset, \mathcal{B})$ are valid for $\mathcal{M}$ due to the same reason in Remark 1.

3.3.3 Unified Algorithm

After the IG stage, we solve the full MILP in each iteration as Algorithm 1. Here, we present the unified method, progressive integrality outer-inner approx-

Algorithm 3: Integrality Generation Stage

Input: p_{cut}, ϵ_{par}, ϵ_{IG}, max_iter, and $\boldsymbol{x}, \text{LB}, \mathcal{K}^{\text{soc}}$ from the IG stage.
Output: $\boldsymbol{x}$ and obj

Initialize $\mathcal{B} = \emptyset$, $\text{LB}_{\text{old}} = 0$;
while $\frac{\text{LB}_{\text{old}} - \text{LB}}{\text{LB}} > \epsilon_{\text{IG}} \wedge |\mathcal{B}| \neq |\boldsymbol{x}|$ **do**
  Update $\mathcal{B}$ by scores for $\boldsymbol{x}$ from (12);
  Set $\text{LB}_{\text{old}} := \text{LB}$;
  Set LB be the objective value of $\bar{\mathcal{O}}(\mathcal{K}^{\text{soc}}, \emptyset, \mathcal{B})$, and $\boldsymbol{x}, \boldsymbol{y}, \boldsymbol{z}$ be the solution;
  Generate cuts for p_{cut} most violated inequalities;
  Add the cut to $\mathcal{K}^{\text{soc}}$ if it is not ϵ_{par}-parallel to added cuts;
end
return $\boldsymbol{x}, \mathcal{K}^{\text{soc}}, \text{LB}$.

imation (PIOIA), which integrates the LP stage (Algorithm 2), IG stage (Algorithm 3), and outer–inner approximation (Algorithm 1) into a unified method as Algorithm 4.

Algorithm 4: Progressive Integrality Outer-Inner Approximation Method (PIOIA)

Input: ϵ, ϵ_{tol}, p_{cut}, ϵ_{par}, ϵ_{LP}, ϵ_{IG} δ_{mip}, max_iter, and t_{solver}.
Output: $\boldsymbol{x}$ and obj

Initialize $\mathcal{K}^{\text{soc}} = \emptyset$, $\mathcal{K}^{\text{cap}} = \emptyset$, $\mathcal{B} = \emptyset$, $\text{UB} := +\infty$, $\text{LB} = 0$;
Conduct Algorithm 2 to get $\boldsymbol{x}$ and update $\text{LB}, \mathcal{K}^{\text{soc}}$;
Conduct Algorithm 3 to get $\boldsymbol{x}$ and update $\text{LB}, \mathcal{K}^{\text{soc}}$;
Conduct Algorithm 1 to get $\boldsymbol{x}^*$ and update LB;
return $\boldsymbol{x}^*, \text{UB}$.

3.4 Time-block Benders Cut for Convergence

While the outer–inner framework improves solution quality, convergence can still be slow due to weak lower bounds. To address this, we introduce time-block Benders cuts. The original SOC-NCUC can be rewritten as the following two-stage problem:

$$\begin{aligned} \min \ & \sum_{t \in \mathcal{T}} \sum_{g \in \mathcal{G}} (C_g^{\text{F}} u_{g,t} + C_g^{\text{SU}} y_{g,t} + C_g^{\text{SD}} z_{g,t}) + \Psi \\ \text{s.t.} \ & (2-3), \\ & p_{\cdot,t}^{\text{master}} = p_{\cdot,t}, \\ & \Psi \geq \sum_{t \in \mathcal{T}} \psi_t(p_{\cdot,t}^{\text{master}}), \end{aligned} \tag{13}$$

where

$$\begin{aligned}\psi_t(p^{\text{master}}_{\cdot,t}) = \min \ & \sum_{g\in\mathcal{G}} C^{\text{V}}_g p_{g,t} + \sum_{n\in\mathcal{N}} C^{\text{P}}(p^{\text{U}}_{n,t} + q^{\text{U}}_{n,t} + p^{\text{O}}_{n,t} + q^{\text{O}}_{n,t}) \\ \text{s.t. } & p_{\cdot,t} = p^{\text{master}}_{\cdot,t}, \quad (\pi_{\cdot,t}) \\ & (3h-5).\end{aligned} \tag{14}$$

The variable $\pi_{\cdot,t}$ is the dual variable of $p_{\cdot,t} = p^{\text{master}}_{\cdot,t}$.

Give a solution $p^*_{\cdot,t}$ from the master problem (13), we solve the subproblem (14) and get the optimal value $\psi^*_t = \psi(p^*_{\cdot,t})$ and $\pi^*_{\cdot,t}$. Then we can get Benders optimality cuts [Benders, 1962, Shapiro et al., 2021]:

$$\psi_t \geq \psi^*_t + {\pi^*_{\cdot,t}}^\top (p_{\cdot,t} - p^*_{\cdot,t}), \text{ for all } t \in \mathcal{T}. \tag{15}$$

Benders cut (15) is for a given time period t; thus, we call it *time-block Benders cut*. After we solve the inner approximation $\mathcal{I}(\boldsymbol{x})$ in Algorithm 1, we have the value of p. Hence, we can generate time-block Benders cuts for all time periods $t \in \mathcal{T}$. These cuts are valid for the original SOC-NCUC; thus, we add them to strengthen the outer approximation $\mathcal{O}(\mathcal{K}^{\text{soc}}, \mathcal{K}^{\text{cap}})$ by incorporating information from the dual of the inner SOCP.

3.5 Discussion

We first compare PIOIA with traditional outer approximation (OA) methods (see e.g., [Duran and Grossmann, 1986, Fletcher and Leyffer, 1994, Bonami et al., 2008, Kronqvist et al., 2019, Bienstock and Villagra, 2025]). A standard OA approach iteratively solves the outer approximation$\mathcal{O}(\mathcal{K}^{\text{soc}}, \mathcal{K}^{\text{cap}})$ and progressively adds linear cuts to tighten the relaxation. However, such methods primarily improve LB and typically do not provide a feasible solution until convergence, i.e., when the outer solution satisfies all nonlinear constraints of SOC-NCUC. As a result, OA may require solving a large number of increasingly complex MILPs, leading to a significant computational burden.

To address this limitation, the proposed framework incorporates an inner approximation by fixing binary variables and solving a convex SOCP. This enables the computation of a valid UB early in the algorithm and allows termination based on the relative optimality gap. Moreover, leveraging advanced conic solvers for the inner problem improves numerical robustness and accelerates feasible solution detection.

Despite these advantages, two main computational challenges remain in the outer–inner approximation framework. First, solving a full MILP in each iteration is still expensive due to the combinatorial complexity of integrality constraints. Second, convergence may be slow because a large number of cuts are required to sufficiently tighten the relaxation.

The PIOIA framework addresses these challenges through two key enhancements. First of all, the progressive integrality strategy reduces the computation workload in MILPs, starting from LP relaxation, then partial integrality, and

finally full integrality. This significantly lowers computational effort in early iterations while still strengthening the relaxation. In addition, the time-block Benders cuts incorporate dual information from the inner SOCP to strengthen the outer approximation, improving the lower bound and accelerating convergence.

Overall, the proposed PIOIA framework integrates outer–inner approximation, progressive integrality, and time-block Benders cuts into a unified approach that improves both computational efficiency and scalability for large-scale SOC-NCUC problems. To the best of our knowledge, this is the first progressive integrality strategy integrated within an outer–inner approximation framework for MISOCP.

4 Experiments

4.1 Setup

Test Sets Experiments are conducted on the Central Illinois 200-bus test system and the South Carolina 500-bus test system [Birchfield et al., 2017]. All data can be found in [Flores, 2022, Appendix. E]. We set the number of time periods $T = 24$, i.e., the hours of a day. Furthermore, we set the unserved/over-produced penalty $C^{\mathrm{P}} = 100 \times \max\{C_g^{\mathrm{V}} : g \in \mathcal{G}\}$, and the each area reserves 10% more loads, i.e. $\mathcal{R}^{\mathrm{D}}_{r,t} = 110\% \times (\sum_{n\in\mathcal{R}} p^{D}_{n,t})$.

Software and Hardware All algorithms are implemented in Julia v1.11.5 [Bezanson et al., 2017], and optimization models are built in JuMP v1.28.0 [Lubin et al., 2023]. We use three commercial solvers: Gurobi v12.0.1 [Gurobi Optimization, LLC, 2023], Mosek v11.0.9 [ApS, 2025], and COPT v8.0.3 [Ge et al., 2022]. We conduct all experiments on a desktop running 64-bit Windows 11 with an AMD Ryzen R5-5600G 3.90 GHz CPU (6 physical cores, 12 logical processors) and 32 GB RAM.

Configurations We run all solvers in their default settings, using up to 6 threads (the number of physical cores in the machine). We set the convergence tolerance as $\epsilon = 1e-4$. For Algorithm 1, we follow [Bienstock and Villagra, 2025], i.e., $\delta_{\mathrm{tol}} := 1e-3$, $\epsilon_{\mathrm{tol}} := 1e-5$, $\epsilon_{\mathrm{par}} := \frac{1}{2}e-5$, and $p_{\mathrm{cut}} := 55\%$. Also, the initial MIP gap is set as $\delta_{\mathrm{mip}} = 1\%$, and the initial time limit of the MIP solver is set as $t_{\mathrm{solver}} = 200$ seconds. During the LP stage, the tolerance to lower bound improvement rate is $\epsilon_{\mathrm{LP}} = 5\%$, and during the IG stage, the tolerance is $\epsilon_{\mathrm{IG}} = 1\%$.

Measurements For both solvers and our proposed method, we can get UB, LB, and the optimal value obj*. We consider relative gap Gap and relative optimality gap OptG, where

$$\mathrm{Gap} := \frac{\mathrm{UB} - \mathrm{LB}}{\mathrm{UB}}, \ \mathrm{OptG} := \frac{\mathrm{UB} - \mathrm{obj}^*}{\mathrm{UB}}.$$

The relative gap describes how close the current upper bound and lower bound are, i.e., how far the current solution is from optimality. We note that the optimality does not only mean finding the optimal solution but also proving the optimality. However, industries usually aim to find a feasible near-optimal solution within a limited runtime; thus, we also use the relative optimality gap to measure the gap between the current best solution and the true optimum.

Furthermore, when solving MISOCPs, solvers sometimes get into numerical troubles and hence return a slightly infeasible solution, i.e., the solution violates some constraints slightly. we also compare the maximum violations Vio reported by solvers.

4.2 Methods Comparisons in Central Illinois 200-Bus Test System

We first test solvers and PIOIA in the Central Illinois 200-Bus Test System. In this subsection, we adopt the formulation that considers unserved demands/power shedding, but does not consider over-produced energy, i.e., $p^{\mathrm{O}}_{n,t} = 0$ and $q^{\mathrm{O}}_{n,t} = 0$.

4.2.1 Solver Performances

First, we test three commercial solvers, Gurobi, Mosek, and COPT, in their default settings with a runtime limit of 7200 seconds. We report the used runtime, final Gap, final OptG, and Vio in Table 2. Furthermore, since the solution of Gurobi suffers from a prominent violation, we also test Gurobi by setting "NumericFocus" to 2 or 3 (NF2 or NF3).

Table 2: Performances for commercial solvers

Solver	Gurobi	Gurobi (NF2)	Gurobi (NF3)	Mosek	COPT
Runtime (s)	3394	7200	7200	7200	7200
Gap	0.004%	NA[1]	NA	1.49%	2.18%
OptG	0%	NA	NA	0.54%	0.54%
Vio	1.34e-05	NA	NA	-[2]	4.94e-06

[1] Do not find any feasible solution.
[2] The maximum violation is less than $1e-6$.

Gurobi with default settings is the only solver that closes the relative gap to the target tolerance within the time limit. However, its solution suffers from prominent constraint violations, indicating potential numerical instability. Increasing the numerical robustness parameters (NumericFocus) prevents Gurobi from finding feasible solutions within the time limit.

In contrast, Mosek and COPT demonstrate better numerical stability but fail to achieve the pre-set convergence within 7200 seconds. These results highlight a fundamental trade-off: MIP-based solvers (Gurobi) are effective in closing optimality gaps but may suffer from numerical issues, while conic solvers (Mosek, COPT) are more stable but less effective in handling integrality.

Based on these observations, we use Gurobi with default settings as the baseline in subsequent experiments.

4.2.2 Impact of Algorithmic Components

We evaluate the contribution of each component in the proposed framework under a time limit of 3600 seconds. Specifically, we compare the following methods: M0 (Gurobi), M1 (outer-inner approximation (Algorithm 1)), M2 (LP stage (Algorithm 2) + M1), M3 (PIOIA (Algorithm 4) without Benders cuts), and M4 (PIOIA with Benders cuts).

Table 3 summarizes the results. M1 improves the ability to obtain high-quality solutions (OptG-0) compared to Gurobi, but requires a longer runtime to reduce the optimality gap. Incorporating the LP stage (M2) significantly accelerates convergence by efficiently strengthening the relaxation using LPs instead of MILPs.

The progressive integrality strategy (M3) further improves performance, achieving faster convergence and better solution quality. This confirms that gradually enforcing integrality effectively balances computational cost and relaxation strength.

Finally, adding time-block Benders cuts (M4) substantially improves the lower bound and enables convergence to the target tolerance within 1433 seconds, reducing runtime by 57.8% compared to Gurobi. Although Benders cuts slightly delay the identification of the optimal solution, they significantly enhance overall convergence.

Table 3: Performances for different methods

Methods	Gap-1	Gap-0.1	OptG-0.1	OptG-0	Final Gap	Runtime
M0	952	3151	1300	3372	0.004%	3394
M1	1956	2411	1956	2679	0.074%	3600
M2	966	1840	966	1390	0.073%	3600
M3	834	1507	834	1268	0.075%	3600
M4	840	1433	840	1433	0.007%	1433

Figure 1 further illustrates the convergence behavior. The LP and IG stages provide better initial relaxations, leading to faster gap reduction once feasible solutions are obtained. Overall, these results demonstrate that each component of PIOIA contributes to improved efficiency, and their combination yields the best performance.

4.3 Robust Test in Central Illinois 200-Bus Test System

We evaluate the robustness of the proposed method under different formulations and perturbed load scenarios.

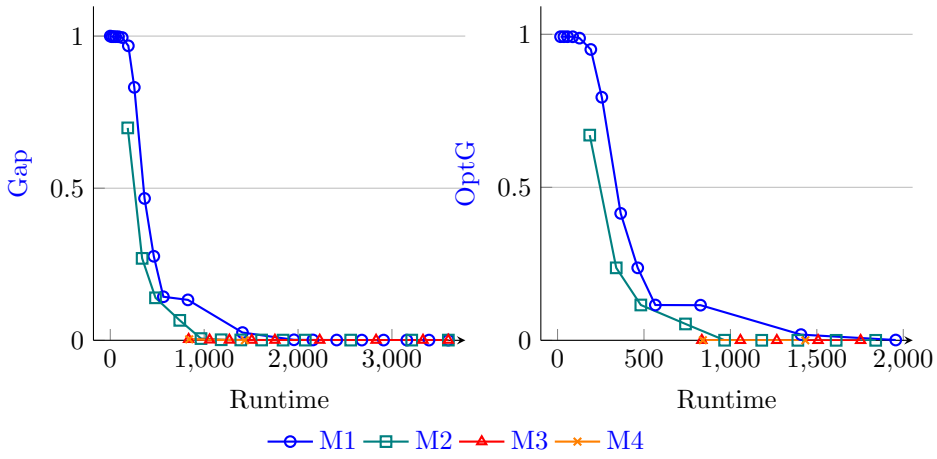

Figure 1: Relative gaps (left graph) and relative optimality gaps (right graph) for different methods

4.3.1 Different Formulations

As we mentioned in Section 2.1, there are three kinds of formulations:

1. Formulation 1 (F1): does not consider slack variables, i.e., $p^{\mathrm{U}}_{n,t} = 0$, $q^{\mathrm{U}}_{n,t} = 0$, $p^{\mathrm{O}}_{n,t} = 0$, and $q^{\mathrm{O}}_{n,t} = 0$.
2. Formulation 2 (F2): only considers the power shedding but not the over-produced energy, i.e., $p^{\mathrm{O}}_{n,t} = 0$, and $q^{\mathrm{O}}_{n,t} = 0$, which has been adopted in the last subsection.
3. Formulation 3 (F3): considers both the power shedding and over-generation.

We note that the optimal values of the three formulations are identical. We test three formulations with a time limit of 3600 seconds.

Table 4 shows that Gurobi's performance varies significantly across formulations and fails to solve one of the formulations, F3. In contrast, M3 consistently finds high-quality solutions across all formulations, demonstrating strong robustness to modeling variations.

4.3.2 Variant Loads

To capture day-to-day variability in demand, we construct perturbed instances by applying small random perturbations to the loads. For the load of each bus n each time t, we perturb it as $(1+\xi) \times p^{\mathrm{D}}_{n,t}$, where ξ is a random variable from a Gaussian distribution $N(0, 0.05^2)$.

In this experiment, we adopt the F2 formulation, 10 random perturbed instances, and a time limit of 3600 seconds. We test M3 and Gurobi. Table 5

Table 4: Performances for Gurobi and M3 in different formulations.

Methods	Gap-1	Gap-0.1	OptG-0.1	OptG-0	Final Gap	Runtime
Gurobi + F1	1497	2362	2207	2664	0.01%	2685
Gurobi + F2	952	3151	1300	3772	0.004%	3394
Gurobi + F3	-	-	-[3]	-	1.11%	3600
M3 + F1	813	1312	813	1148	0.069%	3600
M3 + F2	834	1507	834	1268	0.075%	3600
M3 + F3	723	1381	723	1168	0.057%	3600

[3] The best OptG of Gurobi is 0.14%.

Table 5: Average performances for Gurobi and M3 in variant loads

Methods	Gap-1	Gap-0.1	OptG-0.1	OptG-0	Final Gap	Runtime
Gurobi	894.4	2148.6	1395.6	2814.2	0.021%	3091.3
M3	805.6	1402.8	725.6	1311.2	0.062%	3600

reports average results over 10 instances. The proposed method achieves better solution quality with significantly lower runtime compared to Gurobi.

Moreover, Figure 2 plots the average runtimes for M3 and Gurobi of each feature with a solid line and shaded region for the min–max envelope across samples. It shows that PIOIA exhibits smaller variability across instances, indicating improved stability.

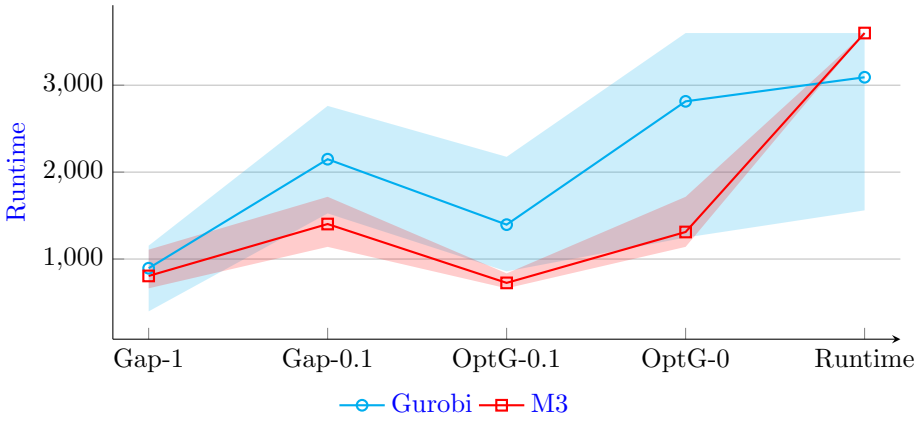

Figure 2: Performance of Gurobi and M3 over 10 random perturbed instances. The solid line shows the mean, and the shaded region represents the min–max envelope across samples.

These results demonstrate that the proposed framework is not only efficient but also robust to modeling choices and data perturbations.

4.4 Case Study in South Carolina 500-Bus Test System

We next evaluate the proposed methods on the larger South Carolina 500-bus system using formulation F2, i.e., allowing power shedding but not over-generation. This case is substantially more challenging computationally and therefore serves as a stronger test of scalability. Gurobi can find the optimal solution in 4519 seconds, with a maximum violation of 1.5×10^{-5}.

We test Gurobi, M2, M3, and M4 with a time limit of 3600 seconds, and Table 6 reports the runtimes required to reach Gap-1, Gap-0.1, OptG-0.1, and OptG-0, together with the final gap and total runtime.

Table 6: Performances for different methods

Methods	Gap-1	Gap-0.1	OptG-0.1	OptG-0	Final Gap	Runtime
Gurobi	1482	-	1503	-	0.11%	3600
M2	1846	2215	1846	2649	0.02%	3600
M3	1558	2049	1558	1558	0.03%	3600
M4	1424	2091	1424	1764	0.005%	2091

The results show that all proposed methods outperform Gurobi in terms of final gap within the prescribed time limit. In particular, M2, M3, and M4 all identify the optimal solution within 3600 seconds, whereas Gurobi does not. Among them, M3 detects the optimal solution fastest, indicating that the progressive integrality strategy remains effective on larger and more challenging instances. Meanwhile, M4 achieves the best overall convergence behavior: although the time-block Benders cuts slightly delay primal convergence compared with M3, they substantially strengthen the lower bound and enable the method to close the relative gap to the target tolerance $\epsilon = 10^{-4}$ in 2091 seconds.

These results confirm that the proposed framework scales effectively to larger systems. In particular, the 500-bus case demonstrates that progressive integrality improves the ability to recover high-quality solutions quickly, while time-block Benders cuts further enhance convergence by tightening the relaxation. Together, these results highlight the practical value of PIOIA for large-scale SOC-NCUC instances.

4.5 Summary of Experiments

Overall, the experimental results demonstrate that the proposed PIOIA framework outperforms state-of-the-art solvers in both efficiency and robustness. By combining outer–inner approximation, progressive integrality, and Benders cuts, the method achieves faster convergence and higher solution quality for large-scale SOC-NCUC problems.

5 Conclusion

In this paper, we proposed PIOIA for solving the SOC-NCUC problem. The proposed approach combines an outer approximation that provides valid lower bounds via MILPs with an inner approximation that detects feasible solutions through convex SOCPs. To improve computational efficiency, we introduced a progressive integrality strategy that gradually enforces integrality, reducing the reliance on expensive MILP solves in early iterations. In addition, time-block Benders cuts were incorporated to strengthen the relaxation and accelerate convergence.

Extensive computational experiments on large-scale test systems demonstrate that the proposed framework significantly improves both efficiency and robustness compared to state-of-the-art commercial solvers. In particular, the progressive integrality strategy enables faster recovery of high-quality feasible solutions, while the Benders cuts enhance convergence by tightening the lower bound. The results on 200-bus and 500-bus systems show that the proposed method scales effectively and remains robust under different formulations and perturbed load scenarios.

Future work includes extending the proposed framework to more complex settings, such as stochastic or robust unit commitment, and integrating additional network models and operational constraints. Another promising direction is to further enhance scalability through parallel implementations and advanced cut management.

References

M. ApS. *The MOSEK Python Fusion API manual. Version 11.0.*, 2025. URL https://docs.mosek.com/latest/pythonfusion/index.html.

Y. Bai, H. Zhong, Q. Xia, C. Kang, and L. Xie. A decomposition method for network-constrained unit commitment with ac power flow constraints. *Energy*, 88:595–603, 2015.

J. Benders. Partitioning procedures for solving mixed-variables programming problems. *Numer. math*, 4(1):238–252, 1962.

K. Bestuzheva, A. Chmiela, B. Müller, F. Serrano, S. Vigerske, and F. Wegscheider. Global optimization of mixed-integer nonlinear programs with scip 8. *Journal of Global Optimization*, pages 287–310, 2025.

J. Bezanson, A. Edelman, S. Karpinski, and V. B. Shah. Julia: A fresh approach to numerical computing. *SIAM review*, 59(1):65–98, 2017.

D. Bienstock and M. Villagra. Accurate linear cutting-plane relaxations for acopf: D. bienstock, m. villagra. *Mathematical Programming Computation*, pages 1–55, 2025.

A. B. Birchfield, T. Xu, K. M. Gegner, K. S. Shetye, and T. J. Overbye. Grid structural characteristics as validation criteria for synthetic networks. *IEEE Transactions on Power Systems*, 32(4):3258–3265, 2017.

P. Bonami, L. T. Biegler, A. R. Conn, G. Cornuéjols, I. E. Grossmann, C. D. Laird, J. Lee, A. Lodi, F. Margot, N. Sawaya, et al. An algorithmic framework for convex mixed integer nonlinear programs. *Discrete optimization*, 5(2):186–204, 2008.

P. Bonami, M. Kilinç, and J. Linderoth. Algorithms and software for convex mixed integer nonlinear programs. In *Mixed integer nonlinear programming*, pages 1–39. Springer, 2011.

M. Carrión and J. M. Arroyo. A computationally efficient mixed-integer linear formulation for the thermal unit commitment problem. *IEEE Transactions on power systems*, 21(3):1371–1378, 2006.

A. Castillo, C. Laird, C. A. Silva-Monroy, J.-P. Watson, and R. P. O'Neill. The unit commitment problem with ac optimal power flow constraints. *IEEE Transactions on Power Systems*, 31(6):4853–4866, 2016.

C. Coffrin, H. L. Hijazi, and P. Van Hentenryck. Strengthening convex relaxations with bound tightening for power network optimization. In *International conference on principles and practice of constraint programming*, pages 39–57. Springer, 2015.

C. Coffrin, H. L. Hijazi, and P. Van Hentenryck. Strengthening the sdp relaxation of ac power flows with convex envelopes, bound tightening, and valid inequalities. *IEEE Transactions on Power Systems*, 32(5):3549–3558, 2016.

A. J. Conejo and L. Baringo. *Power system operations*, volume 11. Springer, 2018.

G. E. Constante-Flores and A. J. Conejo. Security-constrained unit commitment: A decomposition approach embodying kron reduction. *European Journal of Operational Research*, 319(2):427–441, 2024. ISSN 0377-2217.

G. E. Constante-Flores, A. J. Conejo, and F. Qiu. Ac network-constrained unit commitment via relaxation and decomposition. *IEEE Transactions on Power Systems*, 37(3):2187–2196, 2022.

Y. Dai and A. J. Conjeo. Solving the conic formulation of the security-constrained unit commitment problem via decomposition. under review, 2026.

Y. Dai, A. J. Conjeo, and F. Qiu. Scheduling electricity production units to mitigate severe weather impact: An efficient computational implementation. under review, 2025.

M. A. Duran and I. E. Grossmann. An outer-approximation algorithm for a class of mixed-integer nonlinear programs. *Mathematical programming*, 36 (3):307–339, 1986.

R. Fletcher and S. Leyffer. Solving mixed integer nonlinear programs by outer approximation. *Mathematical programming*, 66(1):327–349, 1994.

G. E. C. Flores. *Scheduling of Power Units via Relaxation and Decomposition*. PhD thesis, The Ohio State University, 2022.

A. Frangioni, C. Gentile, and F. Lacalandra. Solving unit commitment problems with general ramp constraints. *International Journal of Electrical Power & Energy Systems*, 30(5):316–326, 2008. ISSN 0142-0615.

T. Gally, M. E. Pfetsch, and S. Ulbrich. A framework for solving mixed-integer semidefinite programs. *Optimization Methods and Software*, 33(3):594–632, 2018.

D. Ge, Q. Huangfu, Z. Wang, J. Wu, and Y. Ye. Cardinal Optimizer (COPT) user guide. https://guide.coap.online/copt/en-doc, 2022.

Gurobi Optimization, LLC. Gurobi Optimizer Reference Manual, 2023. URL https://www.gurobi.com.

D. Han, J. Jian, and L. Yang. Outer approximation and outer-inner approximation approaches for unit commitment problem. *IEEE Transactions on Power Systems*, 29(2):505–513, 2013.

N. J. Higham. *Accuracy and Stability of Numerical Algorithms*. Society for Industrial and Applied Mathematics, second edition, 2002. doi: 10.1137/1.9780898718027.

R. A. Jabr. Radial distribution load flow using conic programming. *IEEE Transactions on Power Systems*, 21(3):1458–1459, 2006.

E. Klotz. Identification, assessment, and correction of ill-conditioning and numerical instability in linear and integer programs. In *Bridging data and decisions*, pages 54–108. INFORMS, 2014.

B. Knueven, J. Ostrowski, and J.-P. Watson. On mixed-integer programming formulations for the unit commitment problem. *INFORMS Journal on Computing*, 32(4):857–876, 2020.

B. Kocuk, S. S. Dey, and X. A. Sun. Strong socp relaxations for the optimal power flow problem. *Operations Research*, 64(6):1177–1196, 2016.

B. Kocuk, S. S. Dey, and X. A. Sun. New formulation and strong misocp relaxations for ac optimal transmission switching problem. *IEEE Transactions on Power Systems*, 32(6):4161–4170, 2017.

J. Kronqvist, D. E. Bernal, A. Lundell, and I. E. Grossmann. A review and comparison of solvers for convex minlp. *Optimization and Engineering*, 20 (2):397–455, 2019.

J. Lavaei and S. H. Low. Zero duality gap in optimal power flow problem. *IEEE Transactions on Power systems*, 27(1):92–107, 2011.

J. Liu, C. D. Laird, J. K. Scott, J.-P. Watson, and A. Castillo. Global solution strategies for the network-constrained unit commitment problem with ac transmission constraints. *IEEE Transactions on Power Systems*, 34(2): 1139–1150, 2018.

M. Lubin, O. Dowson, J. D. Garcia, J. Huchette, B. Legat, and J. P. Vielma. Jump 1.0: recent improvements to a modeling language for mathematical optimization. *Mathematical Programming Computation*, 15:581–589, 2023.

D. K. Molzahn, I. A. Hiskens, et al. A survey of relaxations and approximations of the power flow equations. *Foundations and Trends® in Electric Energy Systems*, 4(1-2):1–221, 2019.

J. A. Muckstadt and S. A. Koenig. An application of lagrangian relaxation to scheduling in power-generation systems. *Operations research*, 25(3):387–403, 1977.

A. Nasri, S. J. Kazempour, A. J. Conejo, and M. Ghandhari. Network-constrained ac unit commitment under uncertainty: A benders' decomposition approach. *IEEE transactions on power systems*, 31(1):412–422, 2015.

J. Ostrowski, M. F. Anjos, and A. Vannelli. Tight mixed integer linear programming formulations for the unit commitment problem. *IEEE transactions on power systems*, 27(1):39–46, 2011.

R. Parker and C. Coffrin. Managing power balance and reserve feasibility in the ac unit commitment problem. *Electric Power Systems Research*, 234:110670, 2024.

I. Quesada and I. E. Grossmann. An lp/nlp based branch and bound algorithm for convex minlp optimization problems. *Computers & chemical engineering*, 16(10-11):937–947, 1992.

J. P. Ruiz, J. Wang, C. Liu, and G. Sun. Outer-approximation method for security constrained unit commitment. *IET Generation, Transmission & Distribution*, 7(11):1210–1218, 2013.

A. Shapiro, D. Dentcheva, and A. Ruszczynski. *Lectures on stochastic programming: modeling and theory*. SIAM, 2021.

D. Tuncer and B. Kocuk. An misocp-based decomposition approach for the unit commitment problem with ac power flows. *IEEE Transactions on Power Systems*, 38(4):3388–3400, 2023.

A. J. Wood, B. F. Wollenberg, and G. B. Sheblé. *Power generation, operation, and control*. John wiley & sons, 2013.

F. Zhuang and F. D. Galiana. Towards a more rigorous and practical unit commitment by lagrangian relaxation. *IEEE Transactions on Power Systems*, 3(2):763–773, 2002.